A Study of Polyhedral Cage Fluxionality in Carboranes. Solution and Solid-State Structures of $R_4C_4B_8H_8$ Isomers[1]

T. Leon Venable, Richard B. Maynard, and Russell N. Grimes*

Contribution from the Department of Chemistry, University of Virginia, Charlottesville, Virginia 22901. *Received May 21, 1984*

Abstract: The reversible cage rearrangement of tetra-C-alkyltetracarbadodecaboranes, $R_4C_4B_8H_8$ (R = CH_3, C_2H_5, or n-C_3H_7), in solution has been examined via ^{11}B, ^{13}C, and ^1H Fourier transform NMR spectroscopy. Each compound exists in solution, in a variety of solvents, as a mixture of two cage isomers designated A and B, with K_{eq} values ([B]/[A] in toluene at 25 °C) of 0.56, 2.2, and 1.9 for the methyl, ethyl, and propyl species, respectively. In the solid state, previous work had shown that the tetramethyl compound exists as isomer A, a distorted icosahedron containing two four-sided open faces. The present study demonstrates that the tetraethyl compound crystallizes as isomer B, which X-ray crystallography establishes as an open framework comprised of two pyramidal C_2B_4 units joined at their basal B–B edges. The tetrapropyl derivative evidently contains both A and B isomers in the solid state. All three compounds, when placed in solution, undergo changes in the [B]/[A] ratio until equilibrium is reached; however, the process is much more rapid in the tetramethyl compound (minutes at 25 °C) than in the higher homologues, which require hours. In each case, removal of solvent causes the compound to revert to its original solid-state cage isomer. From variable-temperature ^{11}B NMR measurements the values of ΔH and ΔS for the A → B conversion, which involves cleavage of a framework C–C bond, were determined to be very small. For ΔH the values range from 1.48 kcal/mol for the tetramethyl to 2.34 for the tetrapropyl derivative, the slight increase being an apparent steric effect. At elevated temperatures, 360-MHz proton NMR data reveal more complex fluxional behavior which has not yielded to analysis. Below room temperature, the A ⇌ B equilibria are observed as low as −80 °C. Observations in polar and nonpolar solvents give no indication of significant solvent effects on the isomerization of any of the three compounds studied. Crystal data for $(C_2H_5)_4C_4B_8H_8$ are as follows: mol wt 258.8; space group $P2_1/n$; $Z = 4$; $a = 7.890$ (2) Å, $b = 17.815$ (6) Å, $c = 12.195$ (9) Å; $\beta = 98.32$ (5)°; $V = 1696$ Å^3; $R = 0.10$ for 1555 reflections having $F_o^2 > 3\sigma(F_o^2)$.

Carboranes containing only carbon and boron in the cage framework do not, as a rule, undergo skeletal rearrangement under mild conditions.[2] True fluxional behavior, involving reversible interconversion of isomers in solution, is even rarer (although examples are known in metallacarborane chemistry[3]). Thus, in the $C_2B_{n-2}H_n$ closo-carborane series, isomerization typically requires elevated temperature, e.g., above 450 °C for conversion of icosahedral 1,2-$C_2B_{10}H_{12}$ to the 1,7 isomer.[2]

In light of this, the remarkable fluxionality exhibited by the 12-vertex $R_4C_4B_8H_8$ carboranes in solution[4,5] has led us to investigate this phenomenon in detail. In the $C_4B_8H_{12}$ system, the presence of 28 skeletal electrons (two more than the optimal number of 26 required for icosahedral geometry,[6] as found in $C_2B_{10}H_{12}$ and $B_{12}H_{12}^{2-}$) leads to distortion of the icosahedral cage. Formally, $C_4B_8H_{12}$ and its colorless, crystalline, air-stable $R_4C_4B_8H_8$ derivatives[8] are of the nido class with $2n + 4$ skeletal electrons, but the actual geometries adopted by 12-vertex, 28-electron boron clusters vary considerably: at least seven distinct types have been established thus far.[9]

Table I. Experimental Parameters and Crystal Data

mol wt	258.8	A[a]	0.70
space group	$P2_1/n$	B[a]	0.35
a, Å	7.890 (2)	2θ range, deg	1.5–47
b, Å	17.815 (6)	reflctns obsd	2022
c, Å	12.195 (9)	reflctns refined	1555
β, deg	98.32 (5)	R	0.10
V, Å^3	1696	R_w	0.11
μ, cm^{-1}	0.5	esd unit wt	2.08
D(calcd), g/cm^3	1.014	Z	4

[a] For explanation see ref 21.

Earlier papers from this laboratory described the synthesis[4,5] of $R_4C_4B_8H_8$ (R = CH_3 or C_2H_5) via oxidative fusion of $R_2C_2B_4H_4^{2-}$ ligands in transition-metal bis(carborane) complexes, X-ray crystallographic studies of the tetra-C-methyl compound[10] and its B-ferrocenyl derivative,[11] and extensive spectroscopic and chemical investigations of the $R_4C_4B_8H_8$ species and their metal derivatives.[4,5] The present study focused on the reversible interconversion of the two isomers (A and B) that are present in solutions of $R_4C_4B_8H_8$ in all solvents examined, where R is CH_3, C_2H_5, or n-C_3H_7, and employed variable-temperature ^{11}B, ^1H, and ^{13}C NMR together with X-ray structural analysis of the tetra-C-ethyl derivative to elucidate these systems.

Results and Discussion

General Observations. The established solid-state structure[10] of $(CH_3)_4C_4B_8H_8$ (**1**) is shown in Figure 1. When placed in solution, the 115.8-MHz proton-decoupled ^{11}B NMR spectrum (Figure 2a) initially is observed to contain four resonances of equal area, consistent with the C_2 symmetry of the solid-state molecular structure; we have designated this species "isomer **A**".[1,5] Within seconds at 25 °C, a new set of peaks corresponding to a second isomer (**B**) appears and increases in intensity until equilibrium

(1) Presented in part at the 183rd National Meeting of the American Chemical Society, Las Vegas, Nevada March 1982, Abstract INOR-140.
(2) (a) Onak, T. P. In "Boron Hydride Chemistry"; Muetterties, E. L., Ed.; Academic Press: New York, 1975, Chapter 10, and references therein. (b) Grimes, R. N. "Carboranes"; Academic Press: New York, 1970. (c) Lipscomb, W. N. "Boron Hydrides"; Benjamin: New York, 1963.
(3) See, for example: Dustin, D. F.; Dunks, G. B.; Hawthorne, M. F. *J. Am. Chem. Soc.* **1973**, *95*, 1109.
(4) For a recent review of work in this area, see: Grimes, R. N. *Adv. Inorg. Chem. Radiochem.* **1983**, *26*, 55.
(5) Maxwell, W. M.; Miller, V. R.; Grimes, R. N. *Inorg. Chem.* **1976**, *15*, 1343.
(6) The Polyhedral Skeletal Electron Pair Theory (PSEPT)[7] predicts stability for closo (fully trianguated) polyhedra having n vertices and $2n + 2$ skeletal electrons and for nido polyhedra (formally derived by removal of a vertex from a closo cage) having n vertices and $2n + 4$ skeletal electrons. CH and BH units contribute 3 and 2 electrons, respectively, to framework bonding.
(7) (a) Wade, K. *Adv. Inorg. Chem. Radiochem.* **1976**, *18*, 1. (b) Mingos, D. M. P. *Nat. Phys. Sci.* **1972**, *236*, 99. (c) Rudolph, R. W. *Acc. Chem. Res.* **1976**, *9*, 446. (d) O'Neill, M. E.; Wade, K. In "Metal Interactions with Boron Clusters"; Grimes, R. N., Ed.; Plenum Press: New York, 1982; Chapter 1 and references therein.
(8) Parent $C_4B_8H_{12}$ has been prepared only in trace quantity (N. S. Hosmane and R. N. Grimes, unpublished results); all investigations to date on C_4B_8 carboranes have utilized C-substituted $R_4C_4B_8H_8$ derivatives.
(9) Maynard, R. B.; Sinn, E.; Grimes, R. N. *Inorg. Chem.* **1981**, *20*, 1201.
(10) Freyberg, D. P.; Weiss, R.; Sinn, E.; Grimes, R. N. *Inorg. Chem.* **1977**, *16*, 1847.
(11) Grimes, R. N.; Maxwell, W. M.; Maynard, R. B.; Sinn, E. *Inorg. Chem.* **1980**, *19*, 2981.

0002-7863/84/1506-6187$01.50/0

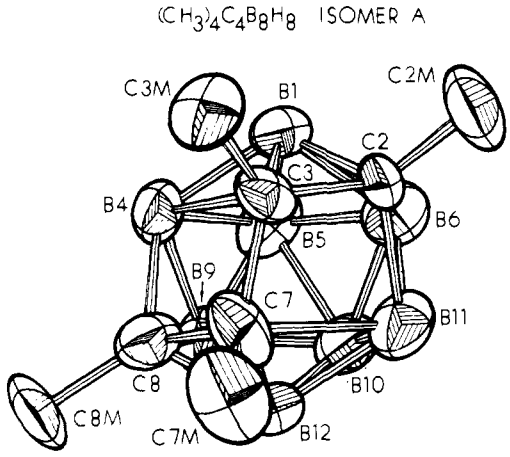

Figure 1. Structure[10] of $(CH_3)_4C_4B_8H_8$.

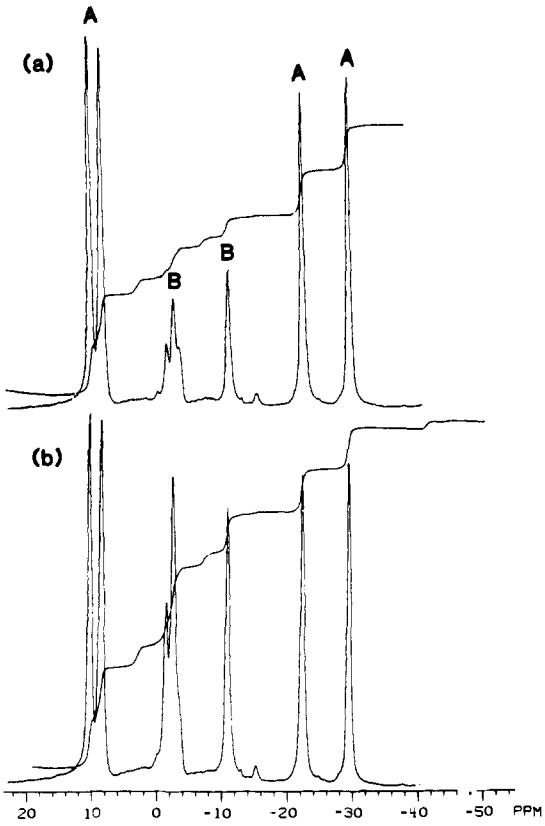

Figure 2. Proton-decoupled ^{11}B NMR spectra (115.8 MHz) of $(CH_3)_4C_4B_8H_8$ in $CDCl_3$ at 25°C: (a) 2 min after dissolving and (b) at equilibrium.

between **1A** and **1B** is established in ca. 20 min (Figure 2b). Isomer **1B** has not been isolated; on removal of solvent, the sample reverts entirely to **1A**, as can be seen by redissolving the material and observing its NMR spectrum. This behavior persists even at low temperature, with no change (other than a broadening of resonances associated with decreased relaxation times) observed in the ^{11}B spectrum down to −80 °C.[5]

The tetra-C-ethyl homologue (**2**) behaves in a generally similar manner, but with a remarkable difference: the solid-state cage structure (**2B**) corresponds to isomer **B** of the tetramethyl compound, and in solution it partially isomerizes (in hours) to an "**A**"-type species (**2A**), as shown in Figure 3. This process is much slower than is the conversion of the tetramethyl species, requiring about 18 h to reach equilibrium. Again, removal of solvent leads to complete conversion back to isomer **B**. Thus, the thermodynamic preference in the solid carboranes shifts from one cage geometry to the other when the methyl groups attached to the cage carbons are replaced by ethyl. The fortuitous circumstance

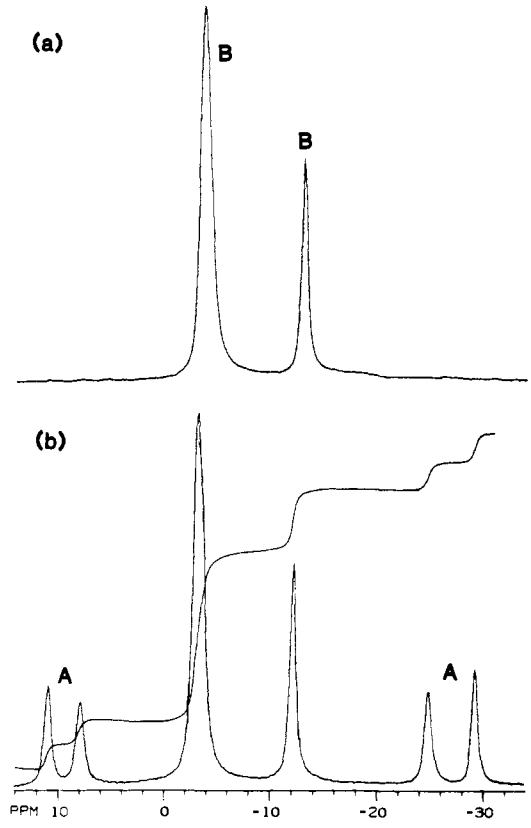

Figure 3. Proton-decoupled ^{11}B NMR spectra (115.8 MHz) of $(C_2H_5)_4C_4B_8H_8$ in $CDCl_3$ at 25 °C: (a) 1 min after dissolving and (b) at equilibrium.

that the tetramethyl and tetraethyl compounds adopt different solid-state isomer structures has permitted the determination of both geometries via X-ray crystallography. This, in turn, allows the interpretation of NMR data for $(alkyl)_4C_4B_8H_8$ species in terms of mixtures of **A** and **B** isomers.

In the case of the tetra-C-*n*-propyl derivative, the situation is more complex in that the solid compound appears to contain two isomers (**3A** and **3B**),[12] the ratio of these species changing, very slowly, when placed in solution (Figure 4); achievement of equilibrium at 25 °C requires about 29 h. It could be argued that the presence of isomers in crystalline **3** arises from rearrangement induced by traces of solvent, but this is highly unlikely given the reproducibility of the ^{11}B NMR spectra of fresh solutions of **3**.

X-ray Diffraction Study of $(C_2H_5)_4C_4B_8H_8$ (2B). Tables I–IV list the crystallographic data collection parameters and crystal data, final positional parameters, and bond distances and angles; for comparison, the corresponding bond lengths for $(CH_3)_4C_4B_8H_8$ (**1A**)[10] and its 4-ferrocenyl derivative[11] are included in Table III. The structure of **2B**, depicted in Figure 5, consists of two $R_2C_2B_4H_4$ units fused together at their basal boron atoms, as does that of **1A** (Figure 1); however, a major difference is found in the central carbon–carbon [C(3)–C(7)] distance, which is clearly nonbonding [2.886 (2) Å] in **2B** but bonding in **1A** (see Table III). Another measure of this difference is given by the angle of tilt between the C_2B_4 pyramids, i.e., the dihedral angle formed by the C(2)–C(3)–B(4)–B(5)–B(6) and the C(7)–C(8)–B(9)–B(10)–B(11) ring planes; this value is virtually zero (0.6°) in the tetramethyl compound[11] but widens to 28.2° in **2B**.

The absence of bonding between C(3) and C(7) in **2B** has direct consequences in the shortening of the remaining C–C distances, C(2)–C(3) and C(7)–C(8), relative to **1A** (Table III). Moreover, it will be noted that the nearby edges C(2)–B(11) and C(8)–B(4) are correspondingly lengthened in **2B**. Thus, the "**B**"-type ge-

(12) The coexistence of two or more isomers in a crystalline solid is unusual but does occur; see: Jeffrey, G. A.; Wood, R. A.; Pfeffer, P. E.; Hicks, K. B. *J. Am. Chem. Soc.* **1983**, *105*, 2128.

Table II. Positional Parameters for $(C_2H_5)_4C_4B_8H_8$

atom	x	y	z
C(2)	0.089 (1)	0.4128 (4)	0.2086 (7)
C(M2)	0.236 (1)	0.4379 (4)	0.1518 (8)
C(E2)	0.289 (2)	0.5211 (5)	0.1669 (10)
C(3)	0.104 (1)	0.3923 (4)	0.3172 (7)
C(M3)	0.277 (1)	0.3897 (5)	0.3962 (8)
C(E3)	0.285 (1)	0.4408 (6)	0.4928 (9)
C(7)	−0.019 (1)	0.2669 (4)	0.1781 (7)
C(M7)	0.098 (1)	0.2059 (4)	0.1495 (9)
C(E7)	0.286 (1)	0.2226 (6)	0.1874 (11)
C(8)	−0.092 (1)	0.2682 (4)	0.2769 (8)
C(M8)	−0.074 (1)	0.2054 (5)	0.3633 (8)
C(E8)	−0.198 (2)	0.1434 (5)	0.3367 (11)
B(1)	−0.032 (2)	0.4641 (5)	0.2901 (10)
B(4)	−0.075 (1)	0.3747 (6)	0.3598 (10)
B(5)	−0.234 (1)	0.4241 (5)	0.2613 (10)
B(6)	−0.102 (1)	0.4349 (5)	0.1473 (9)
B(9)	−0.260 (1)	0.3251 (5)	0.2765 (9)
B(10)	−0.272 (1)	0.3678 (5)	0.1367 (9)
B(11)	−0.077 (2)	0.3364 (5)	0.1021 (9)
B(12)	−0.230 (1)	0.2737 (6)	0.1500 (10)
H(M21)	0.22 (1)	0.431 (5)	0.070 (7)
H(M22)	0.34 (1)	0.405 (5)	0.172 (8)
H(M31)	0.37 (1)	0.401 (5)	0.344 (8)
H(M32)	0.29 (1)	0.337 (5)	0.421 (7)
H(M81)	−0.09 (1)	0.223 (4)	0.433 (7)
H(M82)	0.06 (1)	0.178 (5)	0.346 (8)
H(M71)	0.09 (1)	0.200 (5)	0.062 (8)
H(M72)	0.06 (1)	0.159 (4)	0.186 (7)
H(E21)	0.40 (1)	0.544 (5)	0.147 (8)
H(E22)	0.25 (1)	0.525 (6)	0.253 (9)
H(E23)	0.19 (2)	0.549 (6)	0.121 (11)
H(E31)	0.23 (1)	0.422 (6)	0.559 (9)
H(E32)	0.42 (1)	0.455 (5)	0.502 (10)
H(E33)	0.22 (1)	0.488 (5)	0.479 (9)
H(E71)	0.37 (1)	0.269 (4)	0.164 (7)
H(E72)	0.41 (1)	0.183 (5)	0.160 (7)
H(E73)	0.27 (1)	0.226 (5)	0.258 (8)
H(E81)	−0.24 (1)	0.114 (5)	0.399 (8)
H(E82)	−0.13 (1)	0.104 (5)	0.296 (8)
H(E83)	−0.29 (1)	0.158 (5)	0.282 (8)
H(1)	−0.03 (1)	0.517 (5)	0.311 (8)
H(4)	−0.07 (1)	0.367 (4)	0.445 (7)
H(5)	−0.33 (1)	0.463 (4)	0.287 (6)
H(6)	−0.09 (1)	0.472 (4)	0.066 (7)
H(9)	−0.35 (1)	0.300 (4)	0.300 (6)
H(10)	−0.39 (1)	0.383 (5)	0.085 (7)
H(11)	−0.03 (1)	0.333 (4)	0.027 (7)
H(12)	−0.35 (1)	0.223 (5)	0.159 (7)

ometry can be described as two distinct C_2B_4 units partially fused at their B–B edges, with short cage C–C distances that are indicative of multiple-bond character; the "**A**" structure, on the other hand, more nearly approximates a single 12-vertex cage system with presumably greater delocalization of the skeletal bonding electrons. Another indication of significantly different bonding and charge distribution in the two structures is given by the high-resolution ^{11}B NMR spectra of $(CH_3)_4C_4B_8H_8$ and $(C_2H_5)_4C_4B_8H_8$, discussed below.

The open geometry of **2B** is closely similar to that established for the cobaltacarboranes 1-(η^5-C_5H_5)$Co(CH_3)_4C_4B_7H_7$[13] and 1,12-(η^5-C_5H_5)$Co_2(CH_3)_4C_4B_6H_6$,[14] whose cage skeletons correspond to that of **2B** with one or both apex BH groups [B(1), B(12)] replaced by $Co(C_5H_5)$. Thus, the nonbonding distance C(3)–C(7) is 2.83 Å in the monocobalt complex,[13b] 2.85 Å in its 12-ethoxy derivative,[13c] and 2.79 Å in the dicobalt species,[14] quite close to the corresponding value in **2B**. Similarly, the framework C–C bond lengths in these cobaltacarboranes are ~1.40 Å, again comparable to those in **2B**. Since the presence of $Co(C_5H_5)$ units in the apical vertices cannot sterically inhibit closure of the cage to form an **A**-type isomer, the stabilization of the open-cage "**B**"

(13) (a) Maxwell, W. M.; Grimes, R. N. *Inorg. Chem.* **1979**, *18*, 2174. (b) Welch, A. J., private communication. (c) Pipal, J. R.; Grimes, R. N. *J. Am. Chem. Soc.* **1978**, *100*, 3083.

(14) Pipal, J. R.; Grimes, R. N. *Inorg. Chem.* **1979**, *18*, 1936.

Table III. Bonded and Nonbonded Distances, Å

	$(C_2H_5)_4$-$C_4B_8H_8$[a]	$(CH_3)_4$-$C_4B_8H_8$[b]	$(CH_3)_4C_4B_8H_7$-$(C_5H_4)Fe(C_5H_5)$[c]
	Bond Distances		
C(2)–C(3)	1.362 (6)	1.43 (1)	1.493 (6)
C(2)–C(M2)	1.506 (7)	1.50 (2)	1.519 (6)
C(M2)–C(E2)	1.543 (6)		
C(2)–B(1)	1.732 (8)	1.66 (1)	1.720 (6)
C(2)–B(6)	1.627 (6)	1.70 (1)	1.653 (8)
C(2)–B(11)	2.181 (6)	1.73 (1)	1.641 (7)
C(3)–C(M3)	1.554 (5)	1.54 (1)	1.516 (6)
C(M3)–C(E3)	1.483 (7)		
C(3)–C(7)	2.886 (2)[d]	1.53 (1)	1.515 (5)
C(3)–B(1)	1.669 (6)	1.70 (1)	1.666 (7)
C(3)–B(4)	1.603 (8)	2.15 (1)	2.251 (6)
C(7)–C(8)	1.408 (7)	1.50 (1)	1.490 (6)
C(7)–C(M7)	1.502 (7)	1.48 (1)	1.518 (6)
C(M7)–C(E7)	1.516 (6)		
C(7)–B(11)	1.574 (6)	2.15 (1)	2.197 (7)
C(7)–B(12)	1.656 (7)	1.62 (1)	1.673 (7)
C(8)–C(M8)	1.530 (6)	1.57 (1)	1.493 (6)
C(M8)–C(E8)	1.481 (6)		
C(8)–B(4)	2.145 (7)	1.69 (1)	1.684 (6)
C(8)–B(9)	1.672 (7)	1.70 (1)	1.677 (7)
C(8)–B(12)	1.763 (6)	1.71 (1)	1.695 (7)
B(1)–B(4)	1.859 (7)	1.86 (2)	1.866 (7)
B(1)–B(5)	1.737 (8)	1.84 (2)	1.732 (7)
B(1)–B(6)	1.825 (7)	1.83 (2)	1.748 (8)
B(4)–B(5)	1.832 (6)	1.83 (2)	1.780 (7)
B(4)–B(9)	1.878 (6)	1.82 (1)	1.828 (7)
B(5)–B(6)	1.867 (9)	1.78 (2)	1.708 (8)
B(5)–B(9)	1.788 (6)	1.69 (1)	1.719 (8)
B(5)–B(10)	1.809 (7)	1.80 (1)	1.784 (8)
B(6)–B(10)	1.790 (7)	1.70 (2)	1.733 (9)
B(6)–B(11)	1.859 (6)	1.75 (2)	1.782 (8)
B(9)–B(10)	1.857 (7)	1.80 (2)	1.744 (8)
B(9)–B(12)	1.840 (8)	1.76 (2)	1.771 (8)
B(10)–B(11)	1.744 (8)	1.68 (1)	1.759 (9)
B(10)–B(12)	1.712 (7)	1.76 (2)	1.721 (8)
B(11)–B(12)	1.804 (9)	1.79 (2)	1.819 (9)
⟨B–H⟩	1.090		1.061
⟨C–H⟩	1.036		0.953
	Nonbonded Distances		
C(2)–C(7)	2.743 (7)	2.42 (1)	2.415 (6)
C(3)–C(8)	2.702 (7)	2.39 (1)	2.438 (6)

[a] This work. [b] Reference 10. [c] Reference 11. [d] Nonbonded distance.

Table IV. Selected Bond Angles (deg) in $(C_2H_5)_4C_4B_8H_8$ (**2B**)

C(M2)–C(2)–B(1)	129.15 (32)	C(M7)–C(7)–C(8)	123.57 (38)
C(M2)–C(2)–C(3)	124.14 (33)	C(M7)–C(7)–B(11)	124.66 (48)
C(M2)–C(2)–B(6)	116.08 (34)	C(M7)–C(7)–B(12)	129.93 (33)
C(M2)–C(2)–B(11)	110.41 (33)	C(8)–C(7)–B(11)	111.77 (40)
C(3)–C(2)–B(1)	64.01 (31)	C(8)–C(7)–B(12)	69.73 (35)
C(3)–C(2)–B(6)	117.27 (42)	B(11)–C(7)–B(12)	67.85 (34)
C(3)–C(2)–B(11)	111.91 (29)	C(E7)–C(M7)–C(7)	113.40 (33)
B(1)–C(2)–B(6)	65.75 (29)	C(M8)–C(8)–B(4)	109.23 (34)
B(1)–C(2)–B(11)	109.84 (31)	C(M8)–C(8)–C(7)	124.62 (42)
B(6)–C(2)–B(11)	56.18 (23)	C(M8)–C(8)–B(9)	116.14 (48)
C(E2)–C(M2)–C(2)	116.28 (44)	C(M8)–C(8)–B(12)	128.98 (33)
C(M3)–C(3)–B(1)	128.79 (29)	B(4)–C8)–C(7)	114.39 (33)
C(M3)–C(3)–C(2)	123.83 (41)	B(4)–C(8)–B(9)	57.35 (24)
C(M3)–C(3)–B(4)	121.94 (37)	B(4)–C(8)–B(12)	110.71 (27)
C(2)–C(3)–B(1)	68.82 (32)	C(7)–C(8)–B(9)	115.51 (35)
C(2)–C(3)–B(4)	114.16 (32)	C(7)–C(8)–B(12)	61.78 (31)
B(1)–C(3)–B(4)	69.21 (32)	B(9)–C(8)–B(12)	64.70 (29)
C(E3)–C(M3)–C(3)	114.04 (38)	C(E8)–C(M8)–C(8)	113.68 (34)
C(3)–B(4)–B(5)	104.24 (38)	C(8)–B(9)–B(10)	110.60 (39)
C(3)–B(4)–C(8)	91.07 (36)	B(9)–B(10)–B(11)	99.36 (31)
B(4)–B(5)–B(6)	97.66 (37)	B(10)–B(11)–C(7)	107.53 (45)
B(5)–B(6)–C(2)	102.18 (33)	C(2)–B(11)–C(7)	92.42 (25)

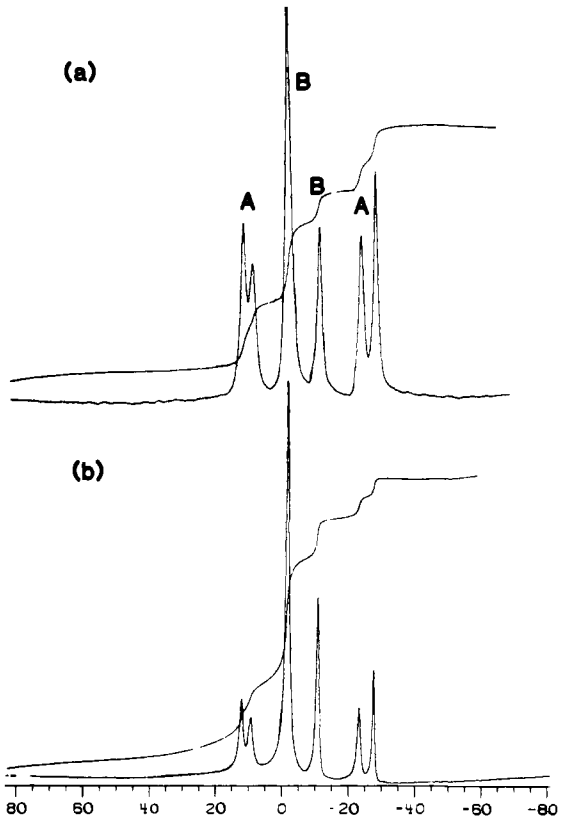

Figure 4. Proton-decoupled ^{11}B NMR spectra (115.8 MHz) of $(n\text{-}C_3H_7)_4C_4B_8H_8$ in $CDCl_3$ at 25 °C: (a) 1 min after dissolving and (b) at equilibrium.

Table V. 115.5-MHz ^{11}B NMR Data (Toluene, 25 °C)

compound	δ^a	J_{BH}, Hz	rel area[b]	δ^a	J_{BH}, Hz	rel area[b]
$(CH_3)_4C_4B_8H_8$ (**1A**)	10.6	171	1	-22.3	159	1
	8.7	216	1	-29.0	147	1
(**1B**)	-1.5	127	1	-10.7	144	1
	-2.3	129	2			
$(C_2H_5)_4C_4B_8H_8$ (**2A**)	11.2	155	1	-24.5	156	1
	8.1	159	1	-28.4	146	1
(**2B**)	-2.4	~144	3	-11.7	143	1
	-3.3	~122				
$(C_3H_7)_4C_4B_8H_8$ (**3A**)	11.4	147	1	-24.3	149	1
	8.6	106	1	-28.2	146	1
(**3B**)	-2.1	122	3	-11.5	138	1

[a] Chemical shifts in ppm relative to $(C_2H_5)_2O{\cdot}BF_3$. [b] Relative peak intensities for a given isomer.

Table VI. Thermodynamic and Kinetic Parameters[a]

	$(CH_3)_4$-$C_4B_8H_8$	$(C_2H_5)_4$-$C_4B_8H_8$	$(C_3H_7)_4$-$C_4B_8H_8$
K_{eq}(25 °C) = [B]/[A]	0.56	2.2	1.9
solid-state isomer	A[b]	B[b]	A + B[c]
first-order rate constant, $10^{-4}k_1$, s^{-1}	4.28 ± 1.52[d]	0.0718 ± 0.0067[e]	0.0247 ± 0.0067[d]
ΔH(A → B),[f] kcal/mol	1.48 ± 0.09	1.84 ± 0.09	2.34 ± 0.26
ΔS(A → B),[f] eu	3.7 ± 0.3	7.3 ± 0.3	9.5 ± 0.8

[a] For experimental data see supplementary material, Tables IX and X. [b] Determined from X-ray crystal structure analysis. [c] Based on the NMR spectrum of fresh solution. [d] For rate of A → B conversion in $CDCl_3$ at 25 °C. [e] For rate of B → A conversion in $CDCl_3$ at 25 °C. [f] Calculated from measurements of K_{eq} between 25 and 100 °C.

geometry in the cobalt complexes is clearly an electronic effect. It is likely that strong covalent bonding between the metal atom(s) and the C_2B_3 face of the carborane ligand reduces the electron density available for trans-facial [C(3)–C(7)] linkage.

^{11}B NMR Studies of Cage Isomerization. For each compound, the ratio of isomers [B]/[A] at any time can be measured from the integrated ^1H-decoupled ^{11}B NMR spectra, in which the **A** and **B** resonances are in each instance clearly distinguishable. In interpreting these spectra, we assume that the **A** isomer of each compound has a "compact" structure (i.e., having a C(3)–C(7) bond) corresponding to that established for **1A**, and similarly, that the **B** form in each species corresponds to the "open" geometry established for **2B** (Figure 6). This premise rests on the close similarity of the ^{11}B chemical shifts for the corresponding isomers in the three compounds, which indicates that we are dealing with qualitatively similar mixtures of cage isomers that differ (except for the identify of the alkyl substituents) only in the [B]/[A] ratio. Further strong evidence is given by the ^1H and ^{13}C NMR spectra of the three carboranes (vide infra).

Table V lists the 115.5-MHz ^{11}B NMR data for the three compounds at 25 °C. In each case, the **A** and **B** resonances are distinguished by changes in peak intensities over time prior to achievement of equilibrium (Figures 2–4 and supplementary material, Tables IX and X). Rates of isomerization and values of K_{eq} (Table VI) were measured for each compound by observing the ^1H-decoupled ^{11}B NMR spectra as a function of time and estimating relative concentrations of **A** and **B** isomers from integrated peak areas.[15] As can be seen, in the tetramethyl species

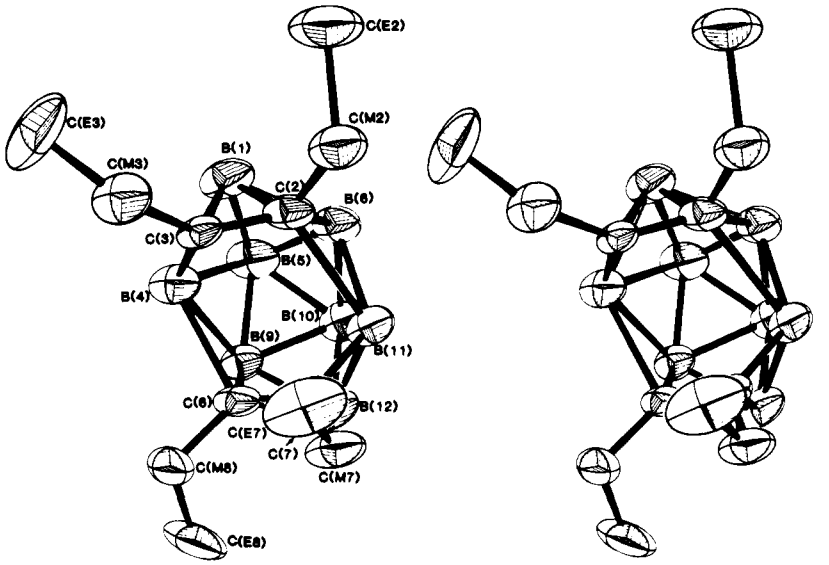

Figure 5. Stereoview of the structure of $(C_2H_5)_4C_4B_8H_8$.

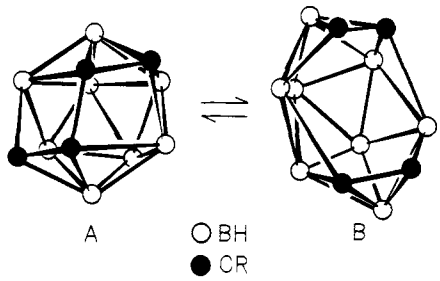

Figure 6. Interconversion of **A** and **B** isomers of $R_4C_4B_8H_8$.

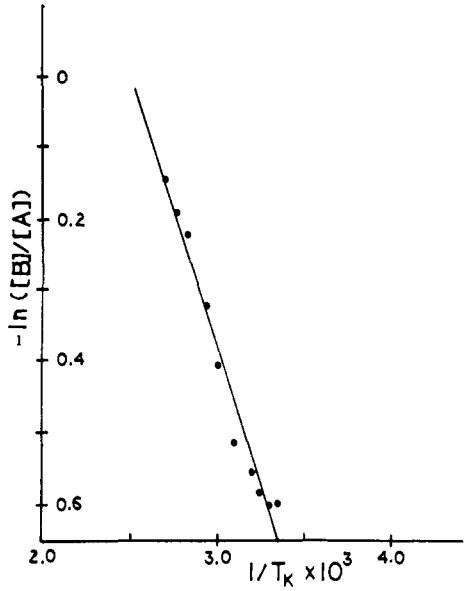

Figure 7. Plot of ln ([B]/[A]) vs. $1/T$ (K) for $(CH_3)_4C_4B_8H_8$ in toluene between 298 and 382 K.

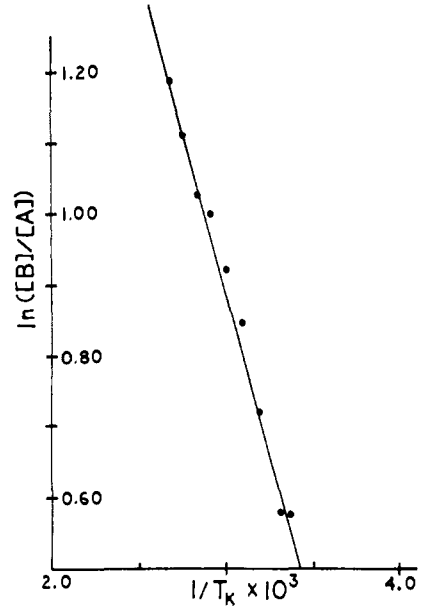

Figure 8. Plot of ln([B]/[A]) vs. $1/T$ (K) for $(C_2H_5)_4C_4B_8H_8$ in toluene between 298 and 382 K.

the **A** form predominates slightly at equilibrium, while in the tetraethyl and tetra-*n*-propyl compounds the **B** isomer is the major component. This can be rationalized in terms of the greater steric bulk of ethyl and propyl groups as opposed to methyl, which can be better accommodated in the open "**B**"-type geometry. However, the fact that K_{eq} in all three systems is relatively close to unity

(15) The error in these measurements is estimated as ±5%.

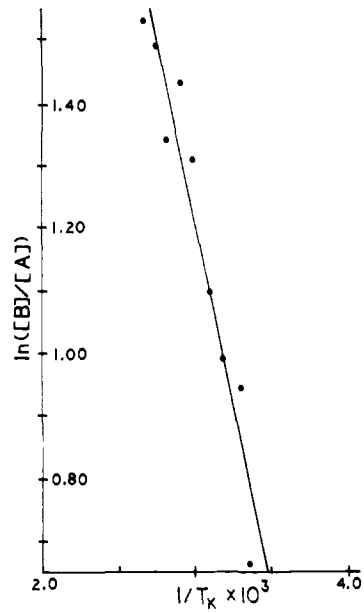

Figure 9. Plot of ln ([B]/[A] vs. $1/T$ (K) for $(n\text{-}C_3H_7)_4C_4B_8H_8$ in toluene between 298 and 382 °K.

Table VII. 90.8-MHz ^{13}C NMR Data (C_6D_6, 25 °C)

compd	δ^a	multiplicity	J_{CH}, Hz
1A	17.55	quartet	130
1B	19.07	quartet	130
2A	25.74	triplet	~127[b]
	25.59	triplet	~127[b]
	15.83	quartet	126
	14.07	quartet	127
2B	29.07	triplet	130
	24.47	triplet	127
	13.49	quartet	~127
	12.21	quartet	128
3A	35.15	triplet	127
	25.07	triplet	127
	23.32	triplet	128
	14.50	quartet	125
	14.29	quartet	125
3B	38.26	triplet	127
	34.90	triplet	128
	22.72	triplet	127
	21.51	triplet	128
	14.60	quartet	125

[a] ppm relative to $(CH_3)_4Si$. [b] Overlapped resonances; measurements are approximate.

indicates that the energy difference between the **A** and **B** forms is quite small. In order to shed further light on these systems, variable-temperature studies were undertaken.

Figures 7–9 depict van't Hoff plots of $1/T$ vs. ln (K_{eq}) between 25 and 100 °C for the three carboranes, based on ^{11}B NMR data which are given in the supplementary material, Table X. In each case, formation of the **B** isomer is favored as the temperature is raised, with small positive values of ΔH indicating that **A** → **B** is an endothermic process; this is as expected since cleavage of the central C–C bond is involved. We interpret the increase in ΔS with increasing size of the alkyl substituents as reflecting an ordering in the solvent sphere in the vicinity of the cage.

Although the data presented here were obtained in toluene solution, statistically identical rate measurements were obtained in $CDCl_3$ at 25 °C; moreover, for all three compounds the observed equilibrium [**B**]/[**A**] ratio at a given temperature does not change noticeably in different solvents. Thus, the **A** ⇌ **B** equilibria are to all intents and purposes solvent independent.

^{13}C and ^1H NMR Spectra. Table VII presents the 90.8-MHz ^{13}C NMR chemical shifts and coupling constants for the **A** and **B** isomers of each carborane. In all cases, the changes in **A** and **B** peak intensities over time parallel those observed in the ^{11}B spectra, and contribute no additional information on the isom-

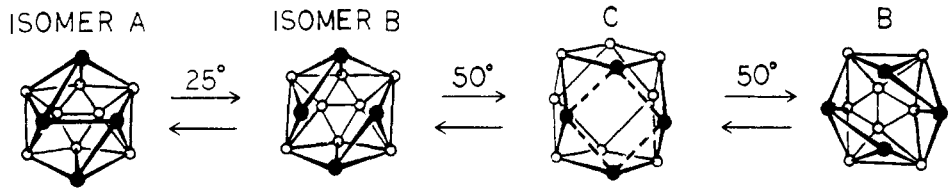

Figure 10. Proposed scheme for interconversion of enantiomers of isomer B at 50 °C.

Table VIII. 360-MHz ^{1}H NMR Data (C_6D_6, 25 °C)

compd	δ	multiplicity[a]	isomer assigned
1	1.62	br s (CH_3)	**A**
	1.70	br s (CH_3)	**A**
	2.01	br s (CH_3)	**B**
	2.07	br s (CH_3)	**B**
2	0.720	t	**B**
	0.893	t	**A, B**
	0.927	t	**A**
	1.725	h	**A**
	2.024	complex; overlapped multiplets	**B**
3	0.673	t	
	0.720	t	
	0.840	t	
	b	*b*	

[a] br s = broad singlet; t = triplet; h = heptet. [b] Complex series of multiplets between δ 1.05 and 2.30.

erization process. The cage carbon resonances, as is typical in carboranes,[16] are weak and partially or wholly obscured by the more intense CH_2 and CH_3 signals. In each instance, the multiplets listed in Table VII can be collapsed to singlets by broadband ^{1}H decoupling.

As previously reported for 100-MHz spectra,[5] the 360-MHz proton spectra of **1** at temperatures above 25 °C reveal additional fluxionality of isomer **1B**, which renders all four cage carbons equivalent on the NMR time scale; thus, at 50 °C in the 100-MHz spectrum the methyl ^{1}H resonances of **1B** coalesce into a singlet. A possible process which accounts for this observation involves breaking the two cage C–C links and forming two new ones, with all B–C bonds remaining intact (Figure 10). This high-temperature rearrangement appears to involve only the **B** isomer, as there are no evident changes in the ^{1}H spectra of **1A** at least up to 50 °C.

The 360-MHz proton spectra of the higher homologues **2** and **3** at 25 °C (Table VIII) have been analyzed in detail and reveal useful information on the structures of these species in solution. The resonance of the alkyl substituents are characterized by strong coupling, the C_2H_5 protons in **2** conforming to an ABX_3 spin system, while the *n*-C_3H_7 substituents in **3** are of the $ABCDX_3$ class. These spin systems indicate that the skeletal carbon atoms are chiral and hence cannot lie on a mirror plane, a conclusion which is consistent with our assumption that the gross solid-state geometries of the **A** and **B** isomers (which contain no mirrors) are maintained in solution.

Above room temperature the proton spectra of **2** and **3** exhibit complex changes which do not involve coalescence of peaks such as those described for **1**. Spectra obtained between 25 and 85 °C in C_6D_6 display small shifts of resonances (1–2 Hz) as the temperature is raised, which are not readily interpretable in terms of structure. It is possible that these observations are temperature-dependent NMR effects that are not related to molecular geometry.

Conclusions

The special properties of 12-vertex, 28-electron $R_4C_4B_8H_8$ species help to illuminate the relation between skeletal electron population and cage geometry, which is one of the fundamental problems in cluster chemistry.[7] When the cage framework is composed solely of boron and carbon, "extra" electrons beyond the 26 required for icosahedral geometry cannot be accommodated except by distortion of the framework; in contrast to transition-metal-containing clusters, there is no opportunity for storage of electrons in nonbonding orbitals.[7d] Yet the inherent tendency of 12-vertex borane frameworks to adopt icosahedral shape is strong. In the $R_4C_4B_8H_8$ system, the net result of these conflicting drives is a close balance between the quasi-icosahedral "**A**" structure and the more open "**B**" geometry. The remarkable near-equality of the **A** and **B** isomers in terms of thermodynamic preference is illustrated in several ways. First, despite the fact that the conversion of **A** to **B** involves cleavage of a C–C link of nominal single-bond length, the observed enthalpy change is only 1–2 kcal/mol, a value nearly two orders of magnitude less than the normal energy (~80 kcal/mol)[17] of such a process. A probable contributing factor in the low ΔH is the relief of strain in the bonds joining the two C_2B_4 units, as the cage opens to form the **B** isomer. Second, the **A–B** equilibrium persists even at −80° C; and third, it is remarkable that replacement of the four CH_3 substituents by C_2H_5 shifts the thermodynamic isomer preference in the solid state from **A** to **B**, while in the *n*-propyl derivative the solid evidently incorporates both isomers. The finding of cage isomerism in the crystalline state is particularly revealing since it must be ascribed to packing forces which are necessarily weak.

In summary, the **A–B** isomer equilibria are so delicately balanced that almost any alteration in the $R_4C_4B_8H_8$ composition is sufficient to tip the scales markedly in one direction or the other. For example, it was noted earlier that replacement of one or both apical BH units with isolobal, electronically equivalent $Co(\eta^5$-$C_5H_5)$ groups gives CoC_4B_7 and $Co_2C_4B_6$ cobaltacarboranes which exhibit the **B**-type geometry only and are nonfluxional.

The behavior of the C_4B_8 carboranes at elevated temperature is complex and involves modes of cage rearrangement that have not been identified in this study. A promising avenue for future investigation would utilize $R_4C_4B_8H_8$ species in which the R group exerts strong electronic influence on the cage structure. An obvious candidate is $(C_6H_5)_4C_4B_8H_8$, whose synthesis has thus far eluded us. Investigations in this area are continuing.

Experimental Section

Instrumentation. NMR spectra were obtained on a Nicolet Magnetics Corporation NT-360/Oxford spectrometer with a 1280/293B data system and variable-temperature control accurate to ±1 °C. Spectra for ^{1}H (361 MHz) and ^{13}C (90.8 MHz) were collected while locked on deuterium (C_6D_6) and referenced to residual C_6D_5H (δ 7.15 relative to tetramethylsilane (Me_4Si)) and $^{13}C_6D_6$ (δ 128.0 relative to Me_4Si) for ^{1}H and ^{13}C, respectively. For ^{13}C spectra the decoupler was turned on between pulses but off during data acquisition so as to provide coupled spectra with Nuclear Overhauser Enhancement (NOE); $^{13}C\{^1H\}$ spectra were collected by using two-level decoupling to minimize sample heating and maintain NOE. The ^{11}B spectra were recorded while either locked on $CDCl_3$ or unlocked (with CH_3–C_6H_5 as the solvent) in a stable (measured drift rate $<2 \times 10^{-3}$ Hz/h) magnetic field with a ^{11}B resonance frequency of 115.8 MHz. Referencing was to an external solution of $(C_2H_5)_2O{\cdot}BF_3$. For $^{11}B\{^1H\}$ spectra, uninterrupted, incoherent decoupling at low levels (~2 W) was employed.

Thermodynamic and kinetic parameters were obtained by a least-squares fit of data from the integration of the ^{11}B spectra.

Materials. The nido-carboranes 2,3-$R_2C_2B_4H_6$ (R = CH_3, C_2H_5, or *n*-C_3H_7) were prepared from B_5H_9 and RC≡CR in the presence of $(C_2H_5)_3N$ as described elsewhere.[18] Conversion of each $R_2C_2B_4H_6$

(16) Wrackmeyer, B. *Prog. NMR Spectrosc.* **1979**, *12*, 227.

(17) Pauling, L. "The Nature of the Chemical Bond"; 3rd ed.; Cornell University Press: Ithaca, New York, 1960; p 85.

(18) (a) Hosmane, N. S.; Grimes, R. N. *Inorg. Chem.* **1979**, *18*, 3294. (b) Maynard, R. B.; Borodinsky, L.; Grimes, R. N. *Inorg. Synth.* **1983**, *22*, 211.

carborane to the corresponding $R_4C_4B_8H_8$ species, via oxidative fusion of the $H_2Fe(R_2C_2B_4H_4)_2$ complex, was conducted by a previously published procedure.[5,19] Characterization data for $H_2Fe[(CH_3)_2C_2B_4H_4]_2$[5,20] and $H_2Fe[(C_2H_5)_2C_2B_4H_4]_2$[19] have been reported earlier. The compound $H_2Fe[(n\text{-}C_3H_7)_2C_2B_4H_4]_2$ (**4**), an air-sensitive red oil obtained in 68% yield (0.551 g) from the reaction of $(n\text{-}C_3H_7)_2C_2B_4H_5^-$ ion with $FeCl_2$ in THF, exhibits an electron-impact mass spectrum with high-mass cutoff at m/e 375, corresponding to that of the $^{56}Fe^{13}C^{12}C_{15}{}^{11}B_8{}^1H_{38}{}^+$ parent ion, and a parent envelope whose relative intensities correspond to the pattern calculated from natural isotopic abundances. A more intense grouping with local cutoff at m/e 317 arises from $(C_3H_7)_4C_4B_8H_8{}^+$ that forms via loss of FeH_2 from **4**. The ^1H-decoupled 115.5-MHz ^{11}B NMR spectrum in C_6D_6 contains peaks at δ -1.1, -7.9, and -19.5 referenced to $(C_2H_5)_2O{\cdot}BF_3$ (relative areas 1:2:1).

X-ray Structure Determination on $(C_2H_5)_4C_4B_8H_8$ (2B). A crystal grown from *n*-hexane solution and mounted on a glass fiber was examined by precession photography and found acceptable. Relevant parameters for the data collection and structure determination are given in Table I. The procedures followed in data collection and processing have been described elsewhere.[21] The space group $P2_1/n$ was determined from systematic absences.

The intensities of three standard reflections showed no greater fluctuations during the data collection than those expected from Poisson statistics. The raw intensity data were corrected for Lorentz-polarization effects but not for absorption. Only those reflections for which $F_o^2 > 3\sigma(F_o^2)$, where (F_o^2) was estimated from counting statistics ($p = 0.03$),[22] were used in the final refinement of the structural parameters, after averaging for equivalent reflections.

Solution and Refinement of the Structure. Full-matrix least-squares refinement was based on F, and the function minimized was $w(|F_o| - |F_c|)^2$. The weights w were taken as $[2F_o/\sigma(F_o^2)]^2$, where $|F_o|$ and $|F_c|$ are the observed and calculated structure factor amplitudes. The atomic scattering factors for non-hydrogen atoms were taken from Cromer and Waber[23] and those for hydrogen from Stewart et al.[24] The effects of anomalous dispersion for all non-hydrogen atoms were included in F by using the values of Cromer and Ibers[25] for $\Delta F'$ and $\Delta f''$.

The MULTAN 74 program series[26] was used to produce a solution of the phase problem, and an E map gave the positions of the 20 non-hydrogen atoms in the asymmetric unit, allowing an unequivocal assignment of atom types to the peaks. Anisotropic temperature factors were introduced for the non-hydrogen atoms. Further Fourier difference functions permitted location of all the nonalkyl, and some alkyl, hydrogen atoms. The remaining alkyl hydrogens were inserted in their calculated positions. The hydrogen atoms were included in the least-squares refinement for several cycles and then held fixed. The model converged to the final R and R_w values given in Table I, where $R = \sum||F_o| - |F_c||/\sum|F_o|$ and $R_w = (\sum w(|F_o| - |F_c|)^2/\sum w|F_o|^2)^{1/2}$. Tables of observed and calculated structure factors and thermal parameters are available as supplementary material. The computing system and programs are described elsewhere.[27]

Acknowledgment. We thank Professor Ekk Sinn for assistance in the X-ray structure determination. This work was supported by the National Science Foundation, Grant No. CHE 81-19936.

Supplementary Material Available: Table IX, measurements of [B]/[A] vs. time for $R_4C_4B_8H_8$ carboranes (R = CH_3, C_2H_5, n-C_3H_7); Table X, measurements of K_{eq} vs. temperature for $R_4C_4B_8H_8$; Table XI, structure factor table for $(C_2H_5)_4C_4B_8H_8$ (12 pages). Ordering information is given on any current masthead page.

(19) Maynard, R. B.; Grimes, R. N. *Inorg. Synth.* **1983**, *22*, 215.
(20) Pipal, J. R.; Grimes, R. N. *Inorg. Chem.* **1979**, *18*, 263.
(21) Finster, D. C.; Grimes, R. N. *J. Am. Chem. Soc.* **1981**, *103*, 2675.
(22) Corfield, P. W. R.; Doedens, R. J.; Ibers, J. A. *Inorg. Chem.* **1967**, *6*, 197.
(23) Cromer, D. T.; Waber, J. T. "International Tables for X-Ray Crystallography"; Kynoch Press: Birmingham, England, 1974; Vol. 4.
(24) Stewart, R. F.; Davidson, E. R.; Simpson, W. T. J. *Chem. Phys.* **1965**, *42*, 3175.
(25) Cromer, D. T.; Ibers, J. A., ref 23.
(26) (a) Main, P.; Woolfson, M. M.; Lessinser, L.; Germain, G.; Declero, J.-P. "Multan 74". (b) Germain, G.; Main, P.; Woolfson, M. M. *Acta Crystallogr., Sect A*, **1971**, *A27*, 368.
(27) Freyberg, D. P.; Mockler, G. M.; Sinn, E. *J. Chem. Soc., Dalton Trans.* **1976**, 447.

Carbon-13 Chemical Shift Tensors of Halobenzenes

B. M. Fung* and C. F. Kong

Contribution from the Department of Chemistry, University of Oklahoma, Norman, Oklahoma 73019. *Received March 21, 1984*

Abstract: The carbon-13 chemical shift tensor of each carbon atom in fluorobenzene, chlorobenzene, bromobenzene, and iodobenzene has been determined. The system used was liquid crystal solutions of the halobenzenes. The anisotropic carbon-13 chemical shifts of the solute in each liquid crystal solution were measured. The ordering factors of the solute molecule were determined from a computer analysis of the proton (and fluorine-19 for fluorobenzene) spectrum. The data of six liquid crystal solutions of each halobenzene were used to calculate the chemical shift tensors. A striking observation is that the tensor component along the C-X axis for the ipso carbon does not change substantially with the substituent in the halobenzenes and in some other mono- and disubstituted benzenes. It was also found that, with the exception of iodobenzene, the tensor component perpendicular to the ring decreases (becomes more shielded) with the separation of the carbon atom from the substituent. This is in contrast to the isotropic shifts, which do not show regular changes with the position of the carbon atom in the ring.

Carbon-13 chemical shifts are very sensitive to the nature of the directly and indirectly bonded atoms and functional groups in a molecule. They have been extensively used in the determination of molecular structures and conformations. A substituent on a benzene ring has a profound effect on the σ- and π-electron densities of all carbon atoms on the ring and can cause substantial changes in chemical properties and reactivities of the compound. An extensive effort has been made to correlate carbon-13 chemical shifts and electron densities and reactivities of substituted benzenes.[1-3] The electronic distributions of aromatic compounds are very anisotropic. Consequently, the chemical shift tensors of aromatic compounds show large anisotropies.[4-10] Obviously the study of the components of the chemical shift tensors would yield more information on molecular structure than the study of the

(1) Bromilow, J.; Brownlee, R. T. C.; Lopez, V. O.; Taft, R. W. *J. Org. Chem.* **1979**, *44*, 4766.
(2) Ewing, D. F. *Org. Magn. Reson.* **1979**, *12*, 499.
(3) Levy, G. C.; Lichter, R. L.; Nelson, G. L. "Carbon-13 Nuclear Magnetic Resonance Spectroscopy", 2nd ed.; Wiley-Interscience: New York, 1980.
(4) Pines, A.; Gibby, M. G.; Waugh, J. S. *Chem. Phys. Lett.* **1972**, *15*, 373.
(5) Pausak, S.; Pines, A.; Waugh, J. S. *J. Chem. Phys.* **1973**, *59*, 591.
(6) Pausak, S.; Tegenfeldt, J.; Waugh, J. S. *J. Chem. Phys.* **1974**, *61*, 1338.
(7) van Dongen Torman, J.; Veeman, W. S. *J. Chem. Phys.* **1978**, *68*, 3233.
(8) Linder, M.; Hohener, A.; Ernst, R. R. *J. Magn. Reson.* **1979**, *35*, 379.
(9) Yarim-Agaev, Y.; Tutunjian, P. N.; Waugh, J. S. *J. Magn. Reson.* **1982**, *47*, 51.
(10) Strub, H.; Beeler, A. J.; Grant, D. M.; Michl, J.; Cutts, P. W.; Zilm, K. W. *J. Am. Chem. Soc.* **1983**, *105*, 3333.

0002-7863/84/1506-6193$01.50/0